Detection and classification of turnouts using eddy current sensors

A. Geistler & F. Böhringer
Institut für Mess- und Regelungstechnik,
University of Karlsruhe, Germany

Abstract

New train operating systems, which allow for a more effective use of track infrastructure, depend on a precise train location. Beyond measuring the vehicle velocity, an eddy current sensor system is able to detect events occurring along the track, e.g. the presence of turnouts. By a classification of turnouts combined with a subsequent map matching, the absolute position of the vehicle on a digital route map can be found without any expensive investment in track infrastructure. This paper presents a method to detect and classify turnouts. Considering the irregularity of the continuous sensor signal, rail clamps and other kinds of events, e.g. turnout components, can be distinguished easily. A characteristic signature is taken from any event, which seems to be a turnout or a turnout component. These signatures are then compared with stored reference data by cross-correlation. Preliminary experiments indicate that a robust detection of an individual type of turnout is possible. Supplemented by the precise distance measurement of the eddy current sensor, the system is suitable for a broad range of railway applications.

1 Introduction

Train-based location of railway vehicles is an important prerequisite for establishing modern railway operating methods. Especially, a reliable odometer function has to be implemented to enable location between given reference points. To avoid an intolerable offset in distance measurement, a recalibration of the odometer has to be performed frequently. The more precise the measurement shall be, the more reference points are necessary. This is conventionally realized by additional infrastructure, e.g. balises. However, a train-borne system with no additional investment in railway infrastructure would clearly be a more attractive solution.

Computers in Railways IX, J. Allan, C. A. Brebbia, R. J. Hill, G. Sciutto & S. Sone (Editors)

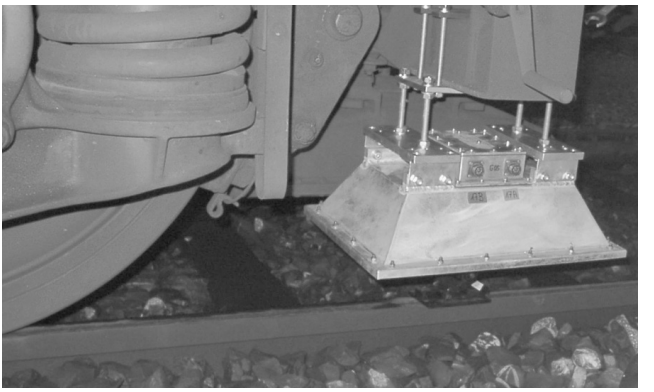

Figure 1: Experimental setup of the eddy current sensor pair.

Common satellite-based systems like the Global Positioning System (GPS) will not work in tunnels or in dense city areas since a direct sight to the satellites is needed. Such drawbacks are avoided by an eddy current sensor system, that evaluates inhomogeneities in magnetic resistance along the rail. This system operates completely automatic on-board and is insensitive to environmental influences, like dust or ice, and allows a robust train location.

2 On-board train location

To provide an exact on-board train location, reliable input data are necessary. On the one hand, the speed and distance measurement has to be as precise as possible. On the other hand, the distance measurement needs fixed reference points to gain an absolute position information of the train. The proposed eddy current sensor system is particularly appealing as it fulfils both tasks [1].

2.1 Sensor system setup

The experimental sensor system setup used for field tests at the *Albtalbahn*, Karlsruhe (Germany) consists of a sensor housing, containing two shielded eddy current sensors [2]. Figure 1 shows the attachment to a bogie of a common railcar.

The developed eddy current sensor system, which is described in [3], is able to detect inhomogeneities in the magnetic resistance along the track. As the sensors are placed at a height of about 100 mm above the rail head, only significant inhomogeneities, e.g. rail clamps or turnout components as well as coarse irregularities of the rail, are detected.

Figure 2 depicts a typical sensor signal in time domain, taken while the train is travelling on vignole rail. The significant inhomogeneities, mainly the rail clamps, can be observed within each sensor channel.

Computers in Railways IX, J. Allan, C. A. Brebbia, R. J. Hill, G. Sciutto & S. Sone (Editors)

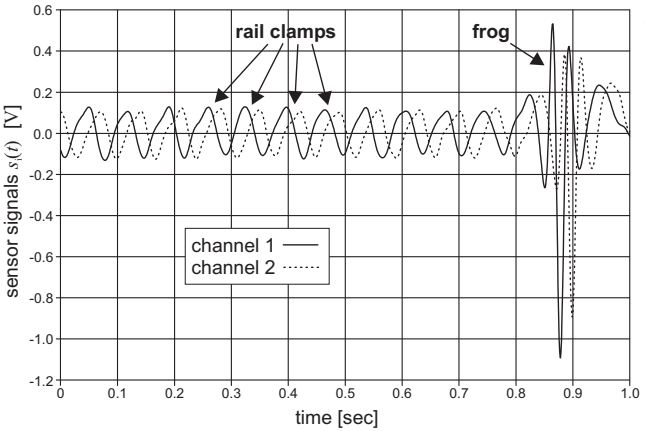

Figure 2: Typical signal of a differential eddy current sensor while travelling on vignole rail.

Figure 2 also shows the different shapes of the sensor signal depending on the parts of the rail the sensor passes. The periodic part of the signal is mainly caused by the rail clamps, as they appear regularly every 60 cm. Most of the turnout components generate signals with significantly larger amplitudes, and their frequency is hardly related to the frequency of the rail clamps. So they contribute mainly to the non-periodic part of the sensor signal.

2.2 Speed and distance measurement

Speed measurement is based upon two individual methods. Firstly, the transit time τ between the two sensor channels is measured by cross-correlation in a closed-loop-correlator (CLC) [2, 3], from which the vehicle velocity

$$v_{\mathrm{CLC}} = \frac{l}{\tau} \tag{1}$$

is obtained, where l denotes the known distance between the two sensors. This measurement has proven accurate and reliable supposing that both signals are well-correlated.

Secondly, the frequency of each sensor channel is analyzed. As can be seen in Fig. 2, the sensor signal mainly reflects the equidistant rail clamps. Since the distance $\overline{x}_{\mathrm{cl}}$ between two adjacent rail clamps is known, locating the maximum in the sensor signal spectrum $f_0 = \arg\max\{|S|^2(f)\}$ corresponds to the frequency of the rail clamps and hence the vehicle velocity can be computed as

$$v_{\mathrm{freq}} = f_0 \cdot \overline{x}_{\mathrm{cl}}\,. \tag{2}$$

Although the frequency analysis provides a less precise velocity measurement, it works with only one signal channel. Thus, the unlikely case of a failure of one

Computers in Railways IX, J. Allan, C. A. Brebbia, R. J. Hill, G. Sciutto & S. Sone (Editors)

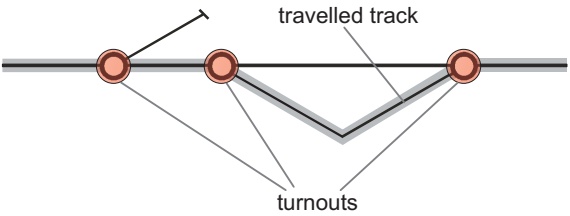

Figure 3: Topological route map.

signal channel does not affect the measurement in a fatal way, since the rail clamp frequency f_0 can still be determined.

Integrating the velocity yields the travelled distance x. To enlarge the robustness, the gained speed data is then fused in a Kalman Filter [4] with an absolute position information obtained from a GPS sensor unit.

2.3 Map matching using topological data

By analyzing track events and matching the data with a digital route map, the speed and distance measurement of the eddy current sensor system becomes more precise, and the absolute position of the rail vehicle can be determined exactly [1, 5]. The digital route map contains information about the location of turnouts and the distance between two neighbouring ones. For train location using the eddy current sensor system, a topological route map as shown in Fig. 3 is sufficient.

Using the proposed setup, it can be decided on which track of a multiple-track line a train is travelling. In addition, the distance measurement of the eddy current sensor system can be improved by eliminating the drift that results from speed integration.

State-of-the-art location systems based on odometry function may only perform location at fixed points along the track that provide an absolute position information. This can be balises, which are installed on the track between or beside the rails. The eddy current sensor system is able to generate a signal, which represents the passed track components. The identification of the passed turnouts and their position yields the input data for the map-matching. The task is now to detect and classify individual turnouts within the continuous eddy current sensor signals.

3 Switch detection and classification

In this section, the different steps to obtain an absolute train position information by detecting and classifying turnouts are presented. To detect a specific event, the signal is segmented into two parts. One contains the signal caused by the rail clamps, which exhibits a known periodicity. The other part contains the events to be detected, i.e. all signal components apart from the frequency of the rail clamps. The detected events, e.g. turnouts, can then be compared with reference data from the digital route map to gain an absolute position information of the train.

Computers in Railways IX, J. Allan, C. A. Brebbia, R. J. Hill, G. Sciutto & S. Sone (Editors)

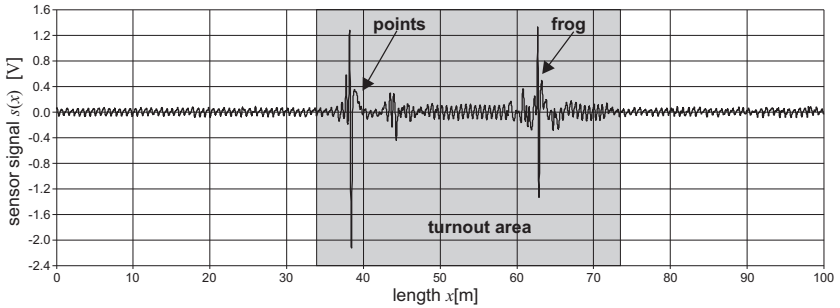

Figure 4: Typical sensor signal in space domain while passing a turnout.

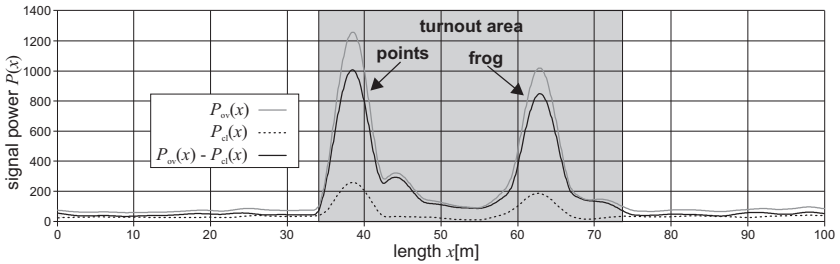

Figure 5: Signal power in space domain while passing a turnout.

3.1 Signal processing

With the vehicle velocity provided by the speed measurement system, the sensor signals are first transformed from time into space domain to eliminate the influence of a varying train velocity. Figure 4 shows a typical sensor signal while passing a facing set of points. In this case, the sensor passes the points first and then the frog.

Passing a turnout, the resulting signals differ significantly from the shape of the signals along open track. The rail clamps appear always with a known frequency f_{cl} in space domain that corresponds to the rail clamp frequency f_0 in time domain, as outlined in Sect. 2.2. Therefore, the signal can be divided into a periodic part, which results from the rail clamps, and a non-periodic part, which results from other parts of the rail, such as turnout components. The average rail clamp frequency f_0 is known from the frequency analysis for the velocity measurement. Thus, using a bandstop filter centered at f_0, signal components near the rail clamp frequency can be suppressed. In space domain, the average frequency of the appearing rail clamps f_{cl} will be at approximately $\frac{1}{0.6\ \mathrm{m}}$.

The overall signal power in space domain $P_{\mathrm{ov}}(x)$ as plotted in Fig. 5 increases significantly while the sensor passes the turnout components. $P_{\mathrm{cl}}(x)$, i.e. the signal power at f_{cl}, is rather low, as the rail clamps in the turnout area often appear at a slightly different average frequency compared to clamps on open track.

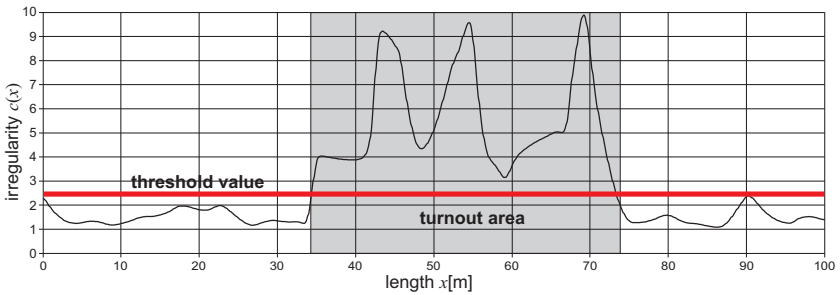

Figure 6: Irregularity of the sensor signal when passing a turnout.

The effect of a higher irregularity and a lower regularity of the sensor signal in areas around special track components is exploited to detect turnouts and other irregular parts of the rail, as illustrated in the following section.

3.2 Switch detection

The characteristic feature of the signals at a turnout is that, compared to the signals on open track, the overall signal power increases significantly while the signal power at the average frequency f_{cl} of the rail clamps decreases. The irregularity

$$c(x) = \frac{P_{\mathrm{ov}}(x) - P_{\mathrm{cl}}(x)}{P_{\mathrm{cl}}(x)} \tag{3}$$

of the signal is defined as the ratio of the power of the irregular part $P_{\mathrm{ov}}(x) - P_{\mathrm{cl}}(x)$ and the power of the regular part at the average frequency of the rail clamps $P_{\mathrm{cl}}(x)$. It is clearly seen in Fig. 5 that this feature allows a reliable detection of events on the track.

Figure 6 depicts the irregularity $c(x)$ on open track and at a turnout in space domain. As the rail clamps are situated slightly closer to each other near the turnout components, the regular part of the signal power is reduced in this area. On the other hand, the irregular part of the signal power is enlarged by the turnout components. Therefore, the irregularity $c(x)$ rises in this case.

In contrast to the overall signal power $P_{\mathrm{ov}}(x)$, the irregularity $c(x)$ is above a chosen threshold value in the whole turnout area so that the turnout can be detected as one event. In case of a strictly constant rail clamp distance $\overline{x}_{\mathrm{cl}}$, the two main components of the turnout, i.e. the points, the frog and the guard rail, respectively, will be detected individually. In addition, any parts of the track, where the rail clamps are not placed at the regular distance $\overline{x}_{\mathrm{cl}}$, can be detected.

3.3 Switch classification

The detected signals according to Sect. 3.2 are compared with stored signal data in the digital route map by cross-correlation methods. The cross-correlation can be

Computers in Railways IX, J. Allan, C. A. Brebbia, R. J. Hill, G. Sciutto & S. Sone (Editors)

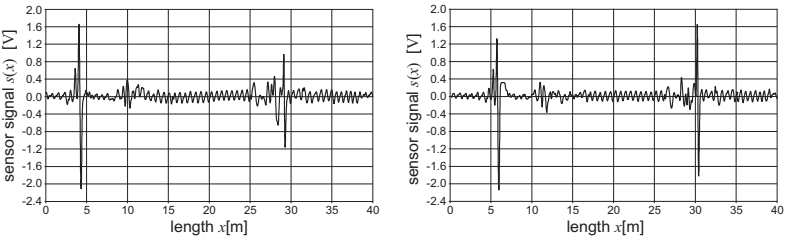

(a) Test run 1. (b) Test run 2.

Figure 7: Sensor signals of the same turnout in different test runs.

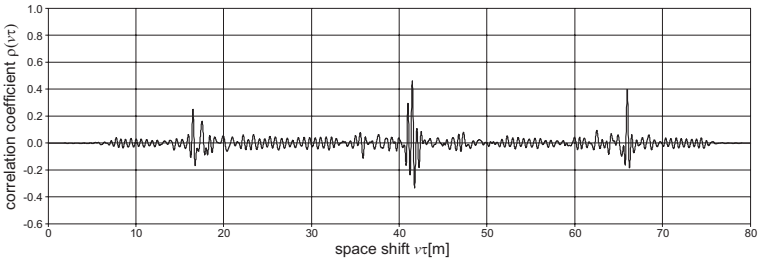

Figure 8: Correlation coefficient using sensor signals in space domain.

conducted using the original sensor signals in space domain, or with a characteristic signature, which has to be generated from the sensor signals.

Figure 7 illustrates the sensor signals in space domain for one particular turnout, taken during two test runs. Figure 7(a) shows the sensor signal taken during test run 1. In the signal, the points appear at a distance from 4 to 8 m, the frog from 26 to 29 m, both with high amplitudes. In Fig. 7(b) the signal recorded during test run 2 is depicted, with the same components visible.

Although both signals look rather similar, there are differences especially at the areas where turnout components appear, mostly with high signal powers. The bogie, where the sensor housing is mounted, is exposed to shocks when the train passes, e.g., a frog. Thus, the maximum correlation coefficient between the two sensor channels may be reduced in these areas [3], as the exact sensor position depends on the bogie movement and therefore also on the train velocity. As a consequence, the maximum of the correlation coefficient $\varrho(v\tau)$, which is depicted in Fig. 8, is at about 45 %.

Instead of correlating the sensor signals directly, signatures of the turnout can be analyzed. The idea is that the signal power is higher at always the same locations, depending on the types of turnout components. Considering a plot of the overall signal power P_{ov}, the similarities between the two test runs are significantly

Computers in Railways IX, J. Allan, C. A. Brebbia, R. J. Hill, G. Sciutto & S. Sone (Editors)

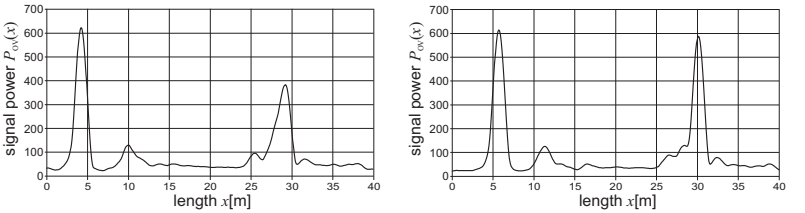

(a) Test run 1. (b) Test run 2.

Figure 9: Measured signal power P_{ov} for two test runs passing the same turnout.

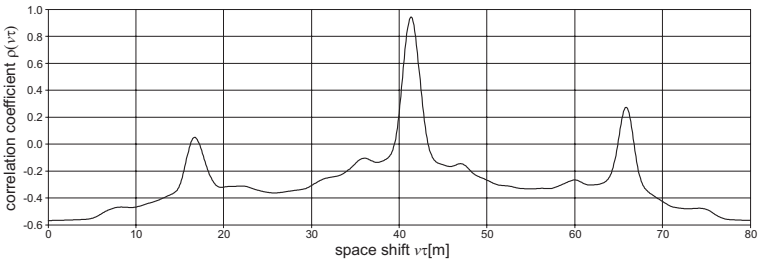

Figure 10: Correlation coefficient using sensor signal power.

enhanced, because phase information and the algebraic sign are neglected. The signature of the same particular turnout is depicted in Fig. 9 for both test runs.

It is worth noting from Fig. 9 that only the position information of turnout components with high signal powers is relevant. This is sufficient to detect turnouts of identical type. The maximum correlation coefficient $\varrho(v\tau)$ rises from 45 % (original signals in space domain) to 95 %. The maxima of the cross-correlation function remain at the same positions. This is depicted in Fig. 10.

Considering different frequency bands of the sensor signal allows to extract different signal power signatures of each turnout. By correlating these signatures, it is possible to detect and classify different types of turnouts. The following parts of the signal power have been considered for taking signatures: The part of the regular signal (rail clamp average frequency) $P_{\mathrm{cl}}(x)$, the overall signal power $P_{\mathrm{ov}}(x)$ and the signal power at frequencies below and above the rail clamp frequency, $P_{\mathrm{h}}(x)$ and $P_{\mathrm{l}}(x)$. The different maximum correlation coefficients $\max\{\varrho_i(v\tau)\}$ as a measure for similarity are combined by multiplication to gain a quality factor

$$Q = \varrho_{\mathrm{cl}} \cdot \varrho_{\mathrm{ov}} \cdot \varrho_{\mathrm{h}} \cdot \varrho_{\mathrm{l}} \,. \tag{4}$$

Preliminary test results showing the robustness of the presented classification method are illustrated in the following section.

Computers in Railways IX, J. Allan, C. A. Brebbia, R. J. Hill, G. Sciutto & S. Sone (Editors)

Table 1: Quality factors for detection and classification of turnout 2.

Test run	Turnout 1	**Turnout 2**	Turnout 3	Turnout 4
1	5.19 %	**71.42 %**	9.30 %	4.02 %
2	4.04 %	**46.29 %**	11.20 %	4.59 %
3	4.02 %	**52.65 %**	9.73 %	4.70 %
Reference	3.10 %	**98.35 %**	6.10 %	1.93 %

Table 2: Quality factors for detection and classification of turnout 3.

Test run	Turnout 1	Turnout 2	**Turnout 3**	Turnout 4
1	5.59 %	2.07 %	**88.40 %**	5.91 %
2	4.25 %	14.29 %	**76.55 %**	8.35 %
3	7.86 %	3.92 %	**79.40 %**	6.46 %
Reference	4.91 %	12.27 %	**97.19 %**	6.45 %

4 Test results

In Tabs. 1 and 2, some results of the turnout classification of several test runs are presented. Table 1 shows the detection and classification of turnout 2 for three test runs. In all test runs, turnout 2 is recognized correctly as the turnout with the highest value of Q. For the calculation of Q, all four signatures have been considered, according to (4). Due to effects of the digital signal processing, especially extracting the turnout area automatically out of the sensor signals, Q is lower than 100 % for the reference data.

The test results for turnout 3 are illustrated in Tab. 2. It can be seen that in each test run turnout 3 is also distinguished reliably from the other reference turnouts.

Turnout 2 shows a slightly higher similarity to turnout 3 than turnout 1 and turnout 4, as they are of the same type but set up in a different direction. Therefore, it is possible to detect and classify type and direction of a turnout and also the position of its points.

5 Conclusion

This contribution has presented an eddy current sensor system for reliable onboard location of trains by detection and classification of turnouts. Correlation of characteristic signatures of turnouts with stored reference data yields the absolute position information of the train. In contrast to location systems based on balises, no additional installation outside the train is needed. The eddy current sensor sys-

Computers in Railways IX, J. Allan, C. A. Brebbia, R. J. Hill, G. Sciutto & S. Sone (Editors)

tem has proved to provide a robust on-board train location. First experiments with natural data from field tests show a high level of accuracy and reliability of the system. This completely autonomous system presents itself to be highly attractive for future train control applications.

Acknowledgements

The authors would like to thank Mr. Frank Ehemann, *Albtal-Verkehrsgesellschaft* (AVG), Karlsruhe, for enabling the field-tests.

References

[1] Geistler, A., Train location with eddy current sensors. *Computers in Railways VIII*, eds. J. Allan, R.J. Hill, C.A. Brebbia, G. Sciutto & S. Sone, WIT Press: Southampton, pp. 1053–1062, 2002.

[2] Engelberg, T., *Geschwindigkeitsmessung von Schienenfahrzeugen mit Wirbelstrom-Sensoren*, Fortschritt-Berichte VDI Reihe 8, Nr. 896. VDI-Verlag: Düsseldorf, 2001.

[3] Engelberg, T. & Mesch, F., Eddy current sensor system for non-contact speed and distance measurement of rail vehicles. *Computers in Railways VII*, eds. J. Allan, R.J. Hill, C.A. Brebbia, G. Sciutto & S. Sone, WIT Press: Southampton, pp. 1261–1270, 2000.

[4] Böhringer, F., Train location based on fusion of satellite and train-borne sensor data. *Location Services and Navigation Technologies*, eds. Y. Zhao, H. A. Klotz Jr. & L.A. Stockum, Proceedings of SPIE, volume 5084, pp. 76-85, 2003.

[5] Mesch, F., Puente León, F. & Engelberg, T., Train-based location by detecting rail switches. *Computers in Railways VII*, eds. J. Allan, R.J. Hill, C.A. Brebbia, G. Sciutto & S. Sone, WIT Press: Southampton, pp. 1251–1260, 2000.

Computers in Railways IX, J. Allan, C. A. Brebbia, R. J. Hill, G. Sciutto & S. Sone (Editors)